International Journal of Pharmaceutics 428 (2012) 125–133

Contents lists available at SciVerse ScienceDirect

International Journal of Pharmaceutics

journal homepage: www.elsevier.com/locate/ijpharm

Adsorption kinetics of plasma proteins on ultrasmall superparamagnetic iron oxide (USPIO) nanoparticles

M. Jansch[a], P. Stumpf[b], C. Graf[b], E. Rühl[b], R.H. Müller[a,*]

[a] Institute of Pharmacy, Department of Pharmaceutics, Biopharmaceutics & NutriCosmetics, Freie Universität Berlin, Kelchstr. 31, 12169 Berlin, Germany
[b] Institute of Chemistry and Biochemistry, Physical and Theoretical Chemistry, Freie Universität Berlin, Takustraße 3, 14195 Berlin, Germany

ARTICLE INFO

Article history:
Received 17 November 2011
Received in revised form 30 January 2012
Accepted 31 January 2012
Available online 8 February 2012

Keywords:
Protein adsorption
2-D PAGE
Drug targeting
Biodistribution
USPIO
Iron oxide nanoparticles

ABSTRACT

In this study the kinetics of plasma protein adsorption onto ultrasmall superparamagnetic iron oxide (USPIO) particles have been analyzed and compared to previously published kinetic studies on polystyrene particles (PS particles), oil-in-water nanoemulsions and solid lipid nanoparticles (SLNs). SPIO and USPIO nanoparticles are commonly used as magnetic resonance imaging (MRI) enhancers for tumor imaging as well as in drug delivery applications. Two-dimensional polyacrylamide gel electrophoresis (2-D PAGE) has been used to determine the plasma protein adsorption onto the citrate/triethylene glycol-stabilized iron oxide surface. The results indicate that the existence of a Vroman effect, a displacement of previously adsorbed abundant proteins, such as albumin or fibrinogen, respectively, on USPIO particles has to be denied. Previously, identical findings have been reported for oil-in-water nanoemulsions. Furthermore, the protein adsorption kinetics differs dramatically from that of other solid drug delivery systems (PS, SLN). More relevant for the in vivo fate of long circulating particles is the protein corona after several minutes or even hours. Interestingly, the patterns received after an incubation time of 0.5 min to 240 min are found to be qualitatively and quantitatively similar. This leads to the assumption of a long-lived ("hard") protein corona around the iron oxide nanoparticles.

1. Introduction

Superparamagnetic iron oxide (SPIO) nanoparticles are widely used in vivo for biomedical applications including magnetic resonance imaging (MRI) contrast enhancement (Fukuda et al., 2006; Peng et al., 2008; Pouliquen et al., 1989) or in drug delivery applications, e.g. loaded with doxorubicin in anti cancer therapy (Gupta and Wells, 2004; Yang et al., 2011). Following intravenous administration, the body distribution of the particles is the most important characteristic as it defines the kind of use. SPIO particles with a size above 50 nm are rapidly phagocytosed by the reticuloendothelial system (RES, i.e. macrophages) and are mostly taken up by the liver (Ferrucci, 1990; Saini et al., 1987). This kind of particles is used as liver-specific MR imaging contrast agents (e.g. Resovist®, Bayer HealthCare Pharmaceuticals, Germany) (Magin et al., 1991; Weissleder et al., 1988). Particles smaller than 50 nm, usually classified as USPIO (ultrasmall superparamagnetic iron oxide nanoparticles), have a lower affinity to the RES and have therefore a longer circulation time within the bloodstream (Saini et al., 1995). Thus, some particles are taken up into the lymph nodes, the bone marrow, the brain, or the spleen. Apart from the particle size of the iron oxide nanoparticles all other physico-chemical properties, such as their surface characteristics, are playing an important role for the in vivo behavior. Variation of these parameters leads to a diverse in vivo fate. Some authors tried to modify the surfaces of the magnetic nanoparticles with PEG to achieve an extended blood half-life by resisting blood protein adsorption (Gupta and Curtis, 2004). Others modified the surface charge of superparamagnetic iron oxide particles and could demonstrate a higher uptake into breast cancer cells by positively charged magnetite nanoparticles compared to negatively charged iron oxide particles (Osaka et al., 2009).

The concept of differential protein adsorption is the key to determine the potential organ distribution (Müller and Heinemann, 1989). Immediately after intravenous application of the nanoparticles, the blood proteins will interact and, depending on the physico-chemical properties of the particles, adsorb onto their surface. Thereby some proteins, such as opsonins, act as a promoter of the phagocytosis and help to detect the particles as foreign material. Typical opsonins are fibrinogen, immunoglobulins and complement proteins (Camner et al., 2002; Leroux et al., 1994). Contrarily, dysopsonins prolong the blood half-life as they inhibit phagocytic

* Corresponding author at: Institute of Pharmacy, Department of Pharmaceutics, Biopharmaceutics & NutriCosmetics, Freie Universität Berlin, Kelchstr. 31, 12169 Berlin, Germany. Tel.: +49 30 83850696; fax: +49 30 83850616.
E-mail addresses: mirko.jansch@gmx.de (M. Jansch), patstu@chemie.fu-berlin.de (P. Stumpf), cmgraf@zedat.fu-berlin.de (C. Graf), ruehl@zedat.fu-berlin.de (E. Rühl), nanoteam@gmx.com (R.H. Müller).

0378-5173/$ – see front matter © 2012 Published by Elsevier B.V.
doi:10.1016/j.ijpharm.2012.01.060

ingestion. Known dysopsonins are e.g. albumin and apolipoproteins (Moghimi et al., 1993; Ogawara et al., 2004).

There are different techniques to identify the adsorbed proteins on the particles surface, such as sodium dodecyl sulfate polyacrylamide gel electrophoresis (SDS-PAGE) (Kang et al., 2007), total internal reflection fluorescence (TIRF) (Jorgensen et al., 2009), shotgun proteomic approach (Capriotti et al., 2011), or combination of atomic force microscopy (AFM), and surface plasmon resonance (SPR) (Servoli et al., 2008). However, two-dimensional polyacrylamide gel electrophoresis (2-D PAGE) is the most powerful one. Up to 10,000 proteins can be determined simultaneously during one sample run (Hochstrasser et al., 1990; Klose and Kobalz, 1995; Tissot et al., 1991). This technique has been optimized for the analysis of adsorbed plasma proteins on polystyrene particles (Blunk et al., 1993), nanoemulsions for parenteral administration (Harnisch and Müller, 1998), solid lipid nanoparticles (SLNs) (Göppert and Müller, 2004), as well as magnetite nanoparticles (Thode et al., 1997).

The adsorption of blood proteins is also time-dependent. Vroman postulated a protein adsorption and displacement onto solid surfaces within a fraction of a second (Vroman and Adams, 1986; Vroman et al., 1980). Abundant proteins with low affinity adsorb first and are subsequently replaced by less plentiful proteins with a higher affinity to the particle surface. This phenomenon is also called "Vroman effect" and might take place within a split second. Blunk et al. (1996) showed the existence of this protein exchange sequence on polymeric model particles. The difficulty in analyzing this early stage of protein adsorption consists of the short incubation time. It is impossible to incubate and separate the particles from unbound plasma within a split second. Therefore, different dilutions of plasma have been used to simulate early stages of protein adsorption without varying the incubation time. A displacement of albumin by fibrinogen and finally of fibrinogen by apolipoproteins was observed. The results are well in agreement with the postulated Vroman effect, since albumin is the most abundant protein in human plasma (albumin 3500–5000 mg/dl; fibrinogen 200–450 mg/dl; apoJ 3.5–10.5 mg/dl). On SLNs Göppert and Müller (2005) observed a transient adsorption of fibrinogen, which was displaced by apolipoproteins. Interestingly, no competitive protein adsorption behavior could be observed on oil-in-water nanoemulsions (o/w nanoemulsions) (Harnisch and Müller, 2000).

The aim of this study was to investigate the kinetics of protein adsorption on USPIO nanoparticles in order to gain a comprehensive understanding of the protein-particle-interactions and to clarify whether there is a Vroman effect on iron oxide nanoparticles or not. A change in the protein adsorption patterns as function of time can also change the organ distribution of the nanoparticles. Furthermore, the impact of prolonged incubation times on the protein adsorption pattern of USPIO nanoparticles has been analyzed. On the hand, early protein adsorption is highly interesting from the academic point of view, on the other hand the sequence of adsorption and desorption processes within a certain period of time is much more relevant to the in vivo behavior of the particles. Particles with a constant protein corona while circulating within the bloodstream can be easily utilized for a targeted use according to the concept of differential protein adsorption (Müller and Heinemann, 1989). The in vivo behavior of an i.v. drug carrier depends on the proteins adsorbed onto its surface which in turn is based on its physicochemical properties. Furthermore, it is likely that an exchange of adsorbed proteins on the particles, which have not been eliminated rapidly by macrophages, occurs during circulation within the bloodstream and leads to a divergent in vivo fate. This will be discussed for USPIO nanoparticles in the second part of this study.

2. Materials and methods

2.1. Synthesis of iron oxide nanoparticles

The synthesis of USPIO nanoparticles in triethylene glycol (TREG) (Sigma–Aldrich, Taufkirchen, Germany) has been carried out according to Cai and Wan (2007). Briefly, tris(acetylacetonato) iron(III), often abbreviated as $Fe(acac)_3$ (Sigma–Aldrich, Taufkirchen, Germany), was mixed with TREG and after a heating and subsequent cooling process an iron oxide nanoparticles dispersion was received. A precipitate of the nanoparticles, induced by adding ethanol and ethyl acetate to the reaction mixture, was magnetically separated from the excess TREG and other by-products using a 1 T permanent magnet in order to obtain a pure black precipitate. Finally, the particles were dispersed in an aqueous sodium citrate solution (200 g/L) (Sigma–Aldrich, Taufkirchen, Germany), stirred for 2 h, and purified by three-fold centrifugation ($4000 \times g$) and redispersion in water or standard infusion solution (Deltajonin) (AlleMan Pharma, Rimbach, Germany). In this way, a stable nanoparticle dispersion in water or standard infusion solution was obtained.

2.2. Characterization of the iron oxide nanoparticles

TEM images were recorded using an EM 902A TEM from Philips (Eindhoven, The Netherlands). The samples were prepared by dipping 400 mesh copper grids coated by a ≈15 nm carbon film (Quantifoil Micro Tools, Jena, Germany) into a dispersion of the nanoparticle samples. Dynamic light scattering measurements were performed on a Delsa Nano C from Beckman Coulter (Krefeld, Germany). At least 10 individual light scattering measurements were performed for deriving the presented averaged values of cumulant fits. IR-spectra were recorded on a Bruker IFS 66/S (Bruker, Karlsruhe, Germany) spectrometer. Raman measurements were performed on a HORIBA Jobin-Yvon Raman microscope linked to a Dilor XY-800 Spektrometer from HORIBA Jobin-Yvon (Lille, France). The exciting wavelength was 532 nm (second harmonic of a Nd:YAG-laser).

2.3. Sample preparation for 2D-PAGE

The sample preparation procedure has been carried out as described earlier (Thode, 1996; Thode et al., 1997). Briefly, particles were incubated in human plasma for 5 min at 37 °C by default. The plasma used in the study was purchased from the center for blood donation (German Red Cross, Berlin, Germany). The nanoparticle dispersion contained of 5.1% (w/w) iron oxide nanoparticles with citrate/TREG stabilization. The standard ratio of iron oxide nanoparticles dispersion to plasma was 1:9 (v/v), similar to previous studies mentioned above. The magnetic properties of the particles have been used to separate unbound plasma proteins from the USPIOs. The sample was placed on top of MS columns, which has been set into the MiniMACS separator (both from Miltenyi Biotec, Bergisch Gladbach, Germany). The magnetic particles were retained in the matrix by magnetic force, implying that the plasma is running through the column. After the excess plasma was washed off, the column was removed from the magnetic field and the particles recovered by elution with 1.5 ml of Milli-Q® water (Fig. 1). The magnetic separation and washing was done again three times to receive a clean sample without unbound plasma proteins. Finally, the volume of the dispersion (1.5 ml) was reduced by centrifugation ($23{,}000 \times g$, 1 h) and the obtained pellet re-dispersed in 30 μl of Milli-Q® water. Removal of adsorbed proteins from the nanoparticles surface has been accomplished by the use of a solubilizing agent containing 10% (w/v) sodium dodecyl sulfate (SDS) and 2.3% (w/v) dithioerythritol (DTE) (Blunk, 1994;

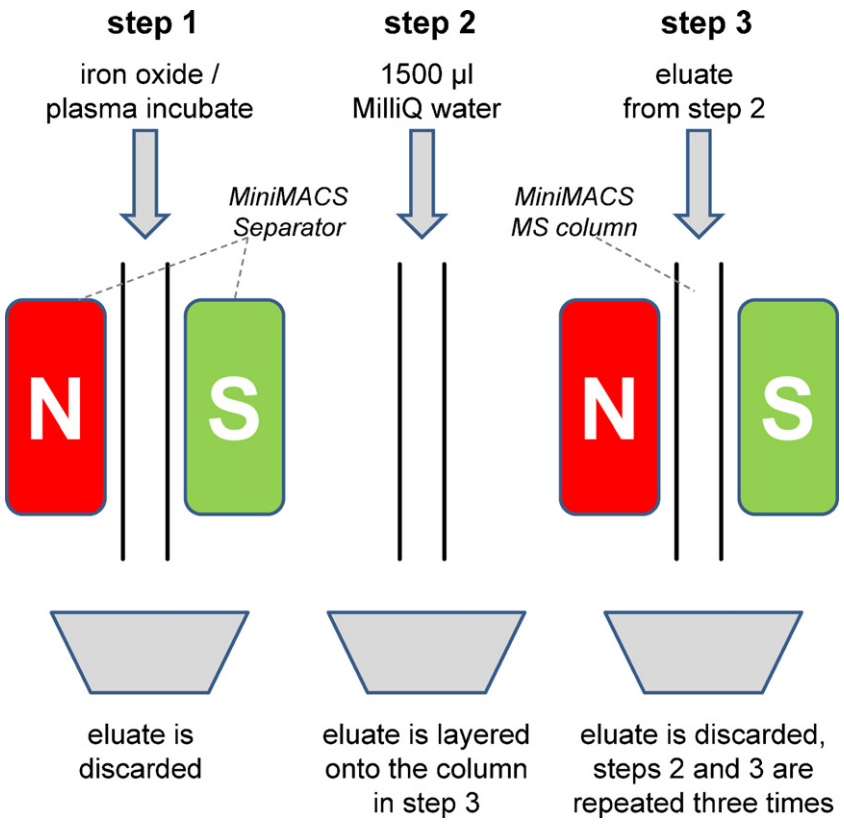

Fig. 1. Schematic drawing of the magnetic separation (see text for further details).

Cook and Retzinger, 1992) followed by the use of a second solution with 4% (w/v) 3-[(3-cholamidopropyl)dimethylammonio]-1-propanesulfonate (CHAPS), 1% (w/v) DTE, 0.5% (w/v) tris (hydroxymethyl) aminomethane and 8 M urea to cover the SDS, which would otherwise disturb the separation process in the first dimension of the gel electrophoresis.

For the study of a possible Vroman effect samples containing of the final amount of 0.9%, 4.5%, 9%, 45% and 90% (v/v) plasma have been prepared. The amount of iron oxide nanoparticles in each sample was constant whereas Milli-Q® water was used for dilution to receive a final ratio of 1:9 iron oxide nanoparticles with citrate/TREG stabilizers (5.1%, w/w) to incubation medium. These concentrations have been chosen according to previously published data (Blunk et al., 1996; Göppert and Müller, 2005; Harnisch and Müller, 2000).

Differing from earlier described sample preparation, the incubation time varied in the second part of this study. With the purpose of a more relevant experimental design of the in vivo behavior of long circulating particles incubation periods of 0.5 min, 5 min, 30 min, and 240 min have been selected. These incubation times are identical with the ones in former kinetic adsorption studies (Blunk et al., 1996; Göppert and Müller, 2005).

2.4. Two-dimensional polyacrylamide gel electrophoresis (2D-PAGE)

The 2D-PAGE analysis has been performed essentially as described previously (Blunk et al., 1993). In the first dimension, isoelectric focusing (IEF), with the Multiphor II (GE Healthcare, Munich, Germany), equipped with a E752 power supply from Consort (Turnhout, Belgium) using 18 cm IPG BlueStrips (Serva, Heidelberg, Germany) with a nonlinear immobilized pH gradient from 3 to 10. For the second dimension, SDS-PAGE, the Protean II xi multi-cell, the Power Pac 1000, the Protean II xi multi-gel casting chamber (18 × 18 × 1.5 mm) and the Model 495 gradient former (all four from Bio-Rad Laboratories, Munich, Germany) were used. The gels employed in this study were cast with a linear gradient from 8 to 16% acrylamide using BIS (N,N′-methylene-bis-acrylamide) as a crosslinker. After the second dimension the gels were silver stained using the Bio-Rad Silver Stain, derived from the method of Merril et al. (1981). The stained gels were scanned with a laser densitometer and were analyzed using the MELANIE software from the Swiss Institute of Bioinformatics (Geneva, Switzerland). Identification of the proteins was accomplished by comparing the spot location with reference maps (ExPASy/SWISS-2DPAGE, Swiss Institute of Bioinformatics, Geneva, Switzerland) (Gasteiger et al., 2003). All other reagents used for 2D-PAGE analysis were of analytical grade and were purchased from Serva (Heidelberg, Germany). All samples have been carried out in duplicates ($n = 2$) due to the time-consuming and expensive technique. A proof of reproducibility has been stated earlier (Blunk, 1994). Therefore, it is in fact not correct to give a standard deviation in the results. However, a Gaussian distribution has been presumed in order to present the results with a standard deviation.

3. Results and discussion

3.1. Early protein adsorption kinetics (Vroman effect) on superparamagnetic iron oxide nanoparticles

When a foreign particle enters the human bloodstream, immediately blood proteins will adsorb to the material surface. Depending on the surface properties certain proteins will predominately attach to it. Furthermore, previously bound proteins might be displaced and other proteins take over their place on the particle surface. This competitive adsorption in plasma has first been

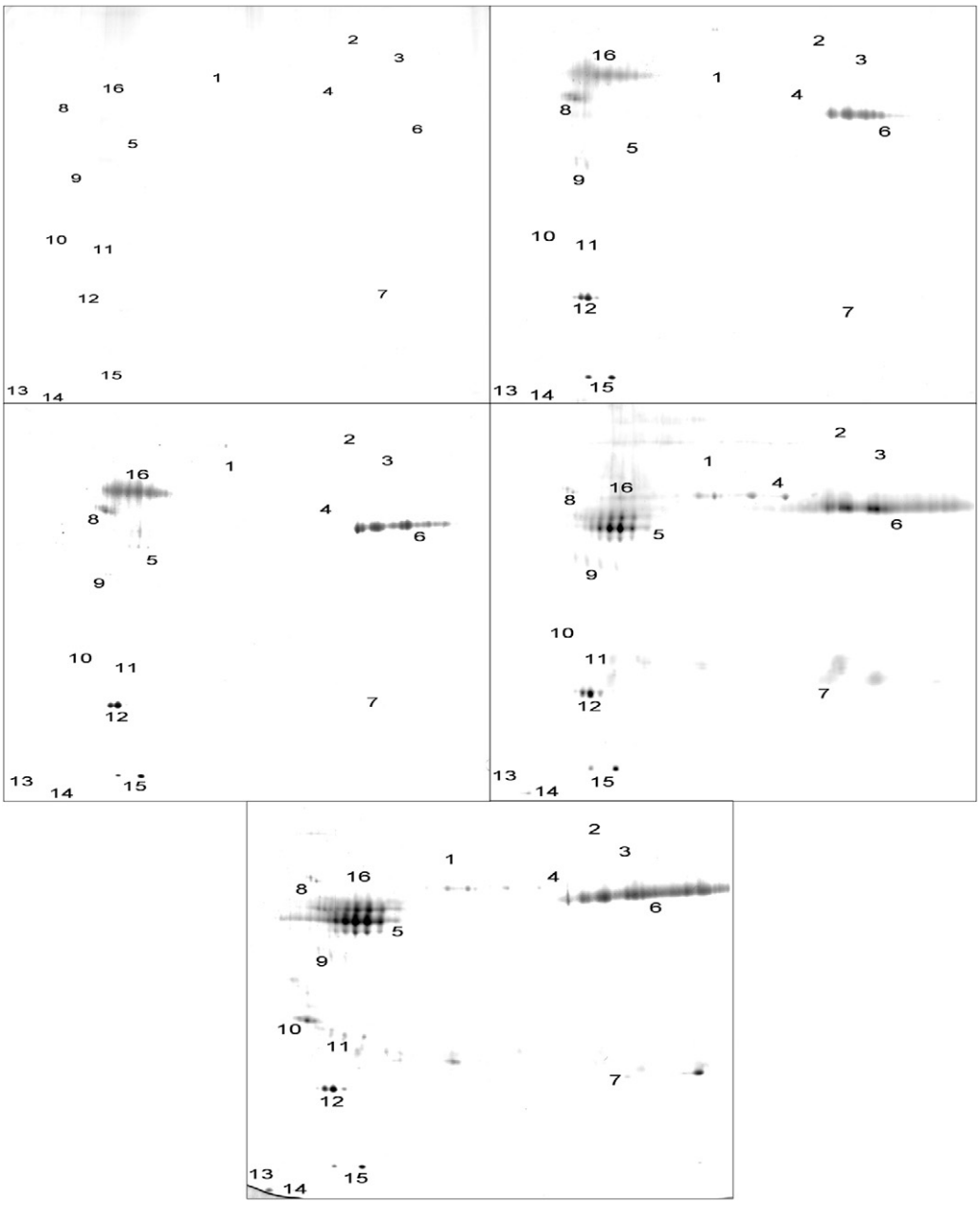

Fig. 2. Plasma protein adsorption patterns of the iron oxide nanoparticles after incubation with 0.9% (top left), 4.5% (top right), 9% (middle left), 45% (middle right), and 90% plasma solution (bottom). (1) Albumin, (2) transferrin, (3) fibrinogen alpha chain, (4) fibrinogen beta chain, (5) fibrinogen gamma chain, (6) immunoglobulin heavy chain gamma, (7) immunoglobulin light chain, (8) alpha-1-antitrypsin, (9) apoA-IV, (10) apoJ, (11) apoE, (12) apoA-I, (13) apoA-II, (14) apoC-II, (15) transthyretin, and (16) immunoglobulin heavy chain alpha.

described by Vroman (1962), therefore it is also called "Vroman effect". In his studies he described a deposit of fibrinogen on varying surfaces (Vroman, 1988; Vroman et al., 1980). A large number of workgroups around the world studied this behavior on different kinds of particles throughout the last decades (Brash and Ten Hove, 1993; Huang et al., 1999; Ihlenfeld and Cooper, 1979).

For polymeric particles, Blunk et al. (1996) could confirm the existence of the Vroman effect using different dilutions of human plasma as incubation medium. Based on the previously used experimental design, Harnisch and Müller (2000) examined the adsorption kinetics on oil-in-water nanoemulsions, concluding there is no displacement of previously adsorbed proteins due to the different chemical nature of the systems. Subsequently, Göppert et al. investigated the adsorption kinetics on solid lipid nanoparticles (SLNs) which consist of a solid matrix, such as polystyrene particles but they are also made of lipids and are therefore chemically very similar to oil-in-water nanoemulsions. Also in this work, a Vroman effect had been observed (Göppert and Müller, 2005).

The iron oxide nanoparticles used in this study can be characterized as follows: TEM measurements yielded an average diameter of 7.8 ± 1.9 nm. The hydrodynamic diameter was 10.7 ± 1.7 nm in water and 12.2 ± 2.1 nm in standard infusion solution. SERS and IR measurements revealed that the composition of the inorganic core of the nanoparticles is a mixture of magnetite (Fe_3O_4) and maghemite (γ-Fe_2O_3).

Fig. 2 shows gel images and Fig. 3 the main groups of proteins, which were generated from adsorption onto the USPIO nanoparticles from diluted plasma with final concentrations of 0.9% (top left), 4.5% (top right), 9% (middle left), 45% (middle right), and 90% plasma solution (bottom). The five adsorption patterns resulted from an

Table 1
Total amount (vol.) and relative volumes (in vol.%) of the most abundant protein species adsorbed on USPIO particles (mean values of two experiments are shown, ± are the standard deviations; $n = 2$).

Adsorbed proteins		"Vroman-kinetics"					Over a period of time			
		0.9% plasma	4.5% plasma	9% plasma	45% plasma	90% plasma	0.5 min	5 min	30 min	240 min
α1-Antitrypsin	vol.	0	596 ± 154	557 ± 184	139 ± 79	133 ± 75	388 ± 139	133 ± 75	724 ± 226	570 ± 33
	vol. (%)	0	9.9 ± 3.8	4.8 ± 0.8	1.3 ± 0.8	0.9 ± 0.4	2.7 ± 0.8	0.9 ± 0.4	2.6 ± 0.2	2.2 ± 0.1
Albumin	vol.	0	84 ± 86	153 ± 50	44 ± 10	149 ± 210	188 ± 108	149 ± 210	234 ± 320	458 ± 70
	vol. (%)	0	1.5 ± 1.6	1.4 ± 0.6	0.4 ± 0.1	1.0 ± 1.3	1.3 ± 0.6	1.0 ± 1.3	0.7 ± 1.0	1.7 ± 0.1
Apolipoprotein A-I	vol.	0	800 ± 175	994 ± 309	790 ± 161	575 ± 93	515 ± 242	575 ± 93	307 ± 43	291 ± 10
	vol. (%)	0	13.3 ± 4.6	8.5 ± 1.3	6.9 ± 0.4	3.9 ± 0.9	3.5 ± 1.5	3.9 ± 0.9	1.1 ± 0.4	1.1 ± 0.1
Apolipoprotein A-II	vol.	0	0	0	76 ± 53	2 ± 3	0	2 ± 3	0	0
	vol. (%)	0	0	0	0.7 ± 0.6	0	0	0	0	0
Apolipoprotein A-IV	vol.	0	153 ± 20	100 ± 11	160 ± 49	40 ± 31	30 ± 26	40 ± 31	139 ± 115	139 ± 11
	vol. (%)	0	2.7 ± 0.3	0.9 ± 0.1	1.5 ± 0.6	0.3 ± 0.2	0.2 ± 0.1	0.3 ± 0.2	0.6 ± 0.5	0.5 ± 0.0
Apolipoprotein C-II	vol.	0	6 ± 7	0	16 ± 22	158 ± 103	0	158 ± 103	9 ± 13	0
	vol. (%)	0	0.1 ± 0.1	0	0.2 ± 0.2	1.1 ± 0.6	0	1.1 ± 0.6	0.1 ± 0.1	0
Apolipoprotein E	vol.	0	0	0	0	128 ± 52	31 ± 28	128 ± 52	285 ± 205	100 ± 22
	vol. (%)	0	0	0	0	1.2 ± 0.8	0.3 ± 0.2	1.2 ± 0.8	1.1 ± 1.0	0.4 ± 0.1
Apolipoprotein J	vol.	0	0	5 ± 7	10 ± 14	331 ± 5	276 ± 91	331 ± 5	1279 ± 8	665 ± 102
	vol. (%)	0	0	0.1 ± 0.1	0.1 ± 0.1	2.2 ± 0.1	1.9 ± 0.7	2.2 ± 0.1	4.7 ± 1.1	2.5 ± 0.2
Fibrinogen α chain	vol.	0	0	7 ± 10	5 ± 7	31 ± 44	79 ± 63	31 ± 44	26 ± 21	98 ± 23
	vol. (%)	0	0	0.1 ± 0.1	0.1 ± 0.1	0.2 ± 0.3	0.5 ± 0.4	0.2 ± 0.3	0.1 ± 0.1	0.4 ± 0.1
Fibrinogen β chain	vol.	0	0	0	524 ± 31	270 ± 39	1035 ± 179	270 ± 39	1943 ± 223	1805 ± 18
	vol. (%)	0	0	0	4.7 ± 0.4	1.8 ± 0.1	7.1 ± 1.6	1.8 ± 0.1	7.2 ± 2.5	6.8 ± 0.6
Fibrinogen γ chain	vol.	0	14 ± 11	577 ± 64	3076 ± 668	5549 ± 209	3981 ± 690	5549 ± 209	7836 ± 639	7137 ± 198
	vol. (%)	0	0.3 ± 0.2	5.0 ± 0.2	26.9 ± 2.1	37.3 ± 4.7	27.3 ± 6.3	37.3 ± 4.7	28.2 ± 4.5	26.8 ± 1.3
Ig light chain	vol.	0	0	281 ± 190	762 ± 25	772 ± 111	1395 ± 325	772 ± 111	2846 ± 90	2746 ± 54
	vol. (%)	0	0	2.3 ± 1.3	6.8 ± 1.1	5.1 ± 0.3	9.6 ± 2.8	5.1 ± 0.3	10.4 ± 2.8	10.3 ± 1.0
Ig heavy chain α	vol.	0	1523 ± 412	2615 ± 115	181 ± 82	0	188 ± 122	0	39 ± 54	9 ± 2
	vol. (%)	0	24.5 ± 3.5	22.8 ± 2.8	1.6 ± 0.5	0	1.3 ± 0.8	0	0.1 ± 0.1	0
Ig heavy chain γ	vol.	0	1857 ± 513	3904 ± 161	3947 ± 495	5727 ± 655	2025 ± 91	5727 ± 655	5794 ± 1036	6949 ± 946
	vol. (%)	0	29.8 ± 4.4	34.0 ± 4.2	34.8 ± 0.5	38.3 ± 0.9	13.8 ± 1.4	38.3 ± 0.9	20.6 ± 1.2	26.0 ± 1.6
Transferrin	vol.	0	0	0	0	0	10 ± 13	0	8 ± 11	288 ± 2
	vol. (%)	0	0	0	0	0	0.1 ± 0.1	0	0	1.1 ± 0.1
Transthyretin	vol.	0	419 ± 46	401 ± 21	348 ± 1	233 ± 12	8 ± 11	233 ± 12	24 ± 34	11 ± 10
	vol. (%)	0	6.8 ± 0.1	3.5 ± 0.4	3.1 ± 0.4	1.6 ± 0.1	0.1 ± 0.1	1.6 ± 0.1	0.1 ± 0.1	0.1 ± 0.1
Total amount	vol.	0	5451 ± 571	9592 ± 1021	10,075 ± 1076	14,095 ± 872	10,145 ± 732	14,095 ± 872	21,489 ± 1551	21,262 ± 1315

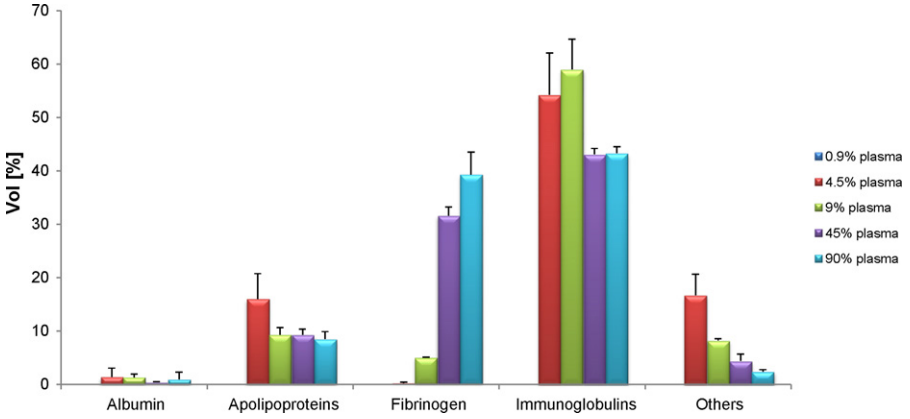

Fig. 3. Relative volume (in vol.%) of the major proteins adsorbed on the surface of superparamagnetic iron oxide nanoparticles obtained from incubation with different plasma dilutions ($n = 2$).

incubation time of 5 min. Table 1 provides a detailed overview of the major adsorbed proteins. No proteins can be detected on the surface of the iron oxide nanoparticles after incubation in the most diluted plasma (0.9%), which corresponds to the very early phase of protein adsorption. A possible explanation for the lack of spotted proteins can be found in the early stage of the adsorption process, which is either caused by the extreme dilution or a detection problem, since the sensitivity of the silver staining is stated to be ~0.1 ng/mm^2. Immunoglobulin (Ig) chains were present in the highest amount (>54% of overall detected proteins) on the adsorption pattern of 4.5% plasma. In addition, there was a considerable amount of apolipoprotein A-I (apoA-I) and smaller fractions of α1-antitrypsin, transthyretin, apoA-IV, and albumin was also detected. Worth mentioning is that nearly no fibrinogen adsorption occurred at this point of time. With increasing plasma concentration the situation changes as the detected amount of fibrinogens rises steadily, reaching up to a maximum of 39.3% of total adsorbed proteins. Overall, fibrinogen is the only protein detected with a permanent increase. Contrarily, the total amount of apolipoproteins is highest at a plasma concentration of 4.5% and decreases with increasing plasma concentration. Generally highest, at all stages of plasma concentration, is the amount of immunoglobulins. Albumin, the most abundant protein in human plasma and therefore, according to Vroman expected to be one of the first proteins adsorbing to the nanoparticles surface, is only present in least amounts on all patterns. This result is well in agreement with a previously published study, where different separation methods have been compared to each other (Thode et al., 1997). Iron oxide nanoparticles have been separated from unbound plasma by means of centrifugation, magnetic separation, gel filtration, and static filtration. The dominant groups of detected proteins are fibrinogen and immunoglobulins, and only minor amounts of albumin have been observed. Nevertheless, one has to keep in mind, the results of the 2-D PAGE technique can be affected by the separation method or the washing medium.

In conclusion, neither a transiently adsorbed fibrinogen nor a complete displacement of a certain protein can be found on the surface of superparamagnetic iron oxide particles. Thus, the patterns show changes but an existence of the Vroman effect on USPIO nanoparticles cannot be documented. From this, the iron oxide nanoparticles are only comparable to the oil-in-water nanoemulsions as they have shown similar characteristics (Harnisch and Müller, 2000). However, a more detailed analysis of the protein corona shows that there are distinct differences between the two systems. Apolipoproteins represented the major group of adsorbed proteins on o/w nanoemulsions. However, they are only playing a minor role in the adsorption process on USPIO particles. Fibrinogen, which is the dominant protein on the citrate/TREG-stabilized iron oxide nanoparticles among immunoglobulins, incubated in high plasma concentrations, showed only a slight affinity to the o/w nanoemulsion surface. Therefore, according to their completely different chemical structure and resulting diverse binding sites, the protein adsorption kinetics is different, as well.

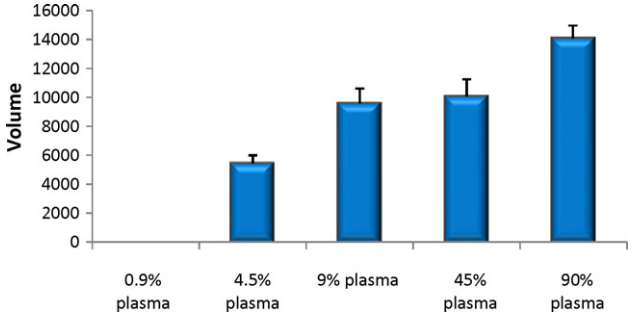

Fig. 4. Total amounts of proteins adsorbed on the surface of the superparamagnetic iron oxide nanoparticles after incubation with different plasma dilutions ($n = 2$).

Fig. 4 shows an overview of the total amounts of adsorbed proteins after incubation in different dilutions of plasma. Generally, an increase of overall amount of adsorbed proteins with increasing plasma concentration can be observed. From 4.5% to 9% plasma concentration, the amount of adsorbed protein is nearly doubled. From 9% to 45%, this quantity is almost constant, and up to 90% plasma concentration, another increase can be detected. A possible explanation can be that saturation of the citrate/TREG-stabilized iron oxide surface with proteins occurs at 9% plasma concentration. Similarly, at 90% plasma concentration there might be a second layer of proteins adsorbed to the surface. This is in agreement with previous work, where multilayer adsorption of blood proteins has been observed and described e.g. on sulfonated polyurethanes (PUs) (Silver et al., 1993).

3.2. Kinetics of plasma protein adsorption on magnetic iron oxide nanoparticles over a certain period of time relevant to drug targeting

The protein adsorption kinetics on superparamagnetic iron oxide nanoparticles after different incubation times were analyzed in order to gain a more comprehensive understanding on the adsorption processes. Intravenously injected particles which are not eliminated rapidly from the bloodstream by macrophages might pass through a sequence of protein adsorption and depletion until a certain uptake occurs (Mientus and Knippel, 1995; Shen et al., 2008). Especially USPIO particles used for extrahepatic

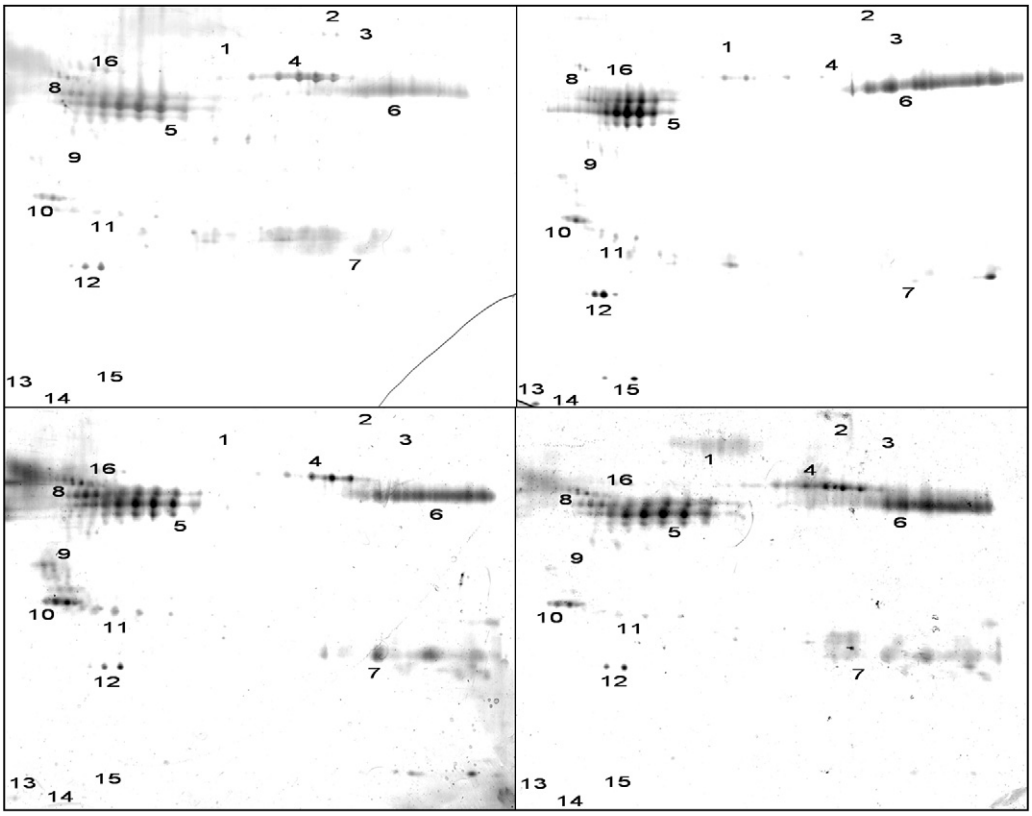

Fig. 5. Plasma protein adsorption patterns of iron oxide nanoparticles after 0.5 min (top left), 5 min (top right), 30 min (bottom left), and 240 min incubation time (bottom right). (1) Albumin, (2) transferrin, (3) fibrinogen alpha chain, (4) fibrinogen beta chain, (5) fibrinogen gamma chain, (6) immunoglobulin heavy chain gamma, (7) immunoglobulin light chain, (8) alpha-1-antitrypsin, (9) apoA-IV, (10) apoJ, (11) apoE, (12) apoA-I, (13) apoA-II, (14) apoC-II, (15) transthyretin, and (16) immunoglobulin heavy chain alpha using a 90% plasma solution.

indications, such as MR lymphography, need to avoid a rapid uptake by liver and spleen (Lind et al., 2002). Besides the particle size, the adsorbed proteins might play the most important role in the fate of the i.v. injected particles (Müller et al., 1997). Lind et al. (2001) could demonstrate that a clear correlation occurs between the protein adsorption data of SPIO particles received by 2-D PAGE and ex vivo from animals.

Based on previous kinetic studies, incubation times of 0.5 min, 5 min, 30 min, and 240 min, were chosen (Blunk et al., 1996; Göppert and Müller, 2005) and the final amount of 90% (v/v) plasma was used as a standard incubation medium. Fig. 5 displays the patterns obtained from different incubation times. With regard to the qualitative aspects of the adsorbed proteins, the four patterns do not differ significantly. Amounts of major proteins, expressed as percentages of the overall protein amount on the particles are presented in Fig. 6 and a more comprehensive compilation of the adsorbed proteins is shown in Table 1.

After 0.5 min incubation time fibrinogen is already the dominant protein adsorbing onto the surface of the iron oxide nanoparticles. This is interesting as it could not be found in the early stages of the Vroman study (cf. Section 3.1). Otherwise, one has to keep in mind, that the Vroman kinetics take place within a split second and in this study the shortest incubation time was 30 s. The relative amount of adsorbed fibrinogen is relatively independent on the incubation

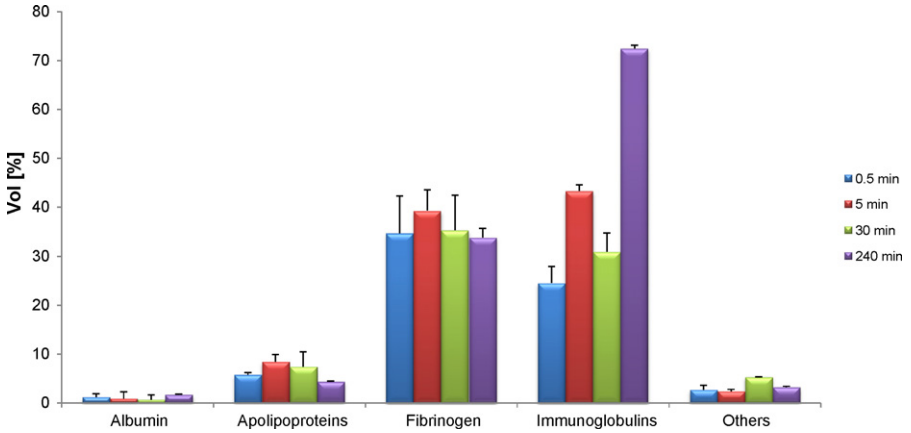

Fig. 6. Relative volume (in vol.%) of major proteins adsorbed onto the surface of superparamagnetic iron oxide nanoparticles obtained from different incubation times ($n = 2$) using a 90% plasma solution.

time, but an absolute increase with raising incubation times can be observed. Also present in relatively high quantities are the immunoglobulins. Likewise fibrinogen, the absolute amount of this adsorbed species increases with incubation time. Both belong to the group of opsonic proteins, accelerating the macrophage detection of the particles as foreign material. Nagayama et al. (2007) analyzed the time-dependent changes of opsonin adsorption onto nanoparticles and their effect on the hepatic uptake. An increased uptake by Kupffer cells has been correlated with an increased adsorption of opsonins, mainly complement C3 and IgG, with an increase of incubation time. Based on these findings a strong accumulation of magnetite nanoparticles in the liver appears to be most likely. Previously, immunoglobulins and fibrinogen have been identified as the major adsorbed proteins on iron oxide particles, which were stabilized once with chondroitin-4-sulfate and others with carboxydextran (Müller et al., 1997). In vivo both types of magnetite nanoparticles showed a quick uptake by Kupffer cells of the liver.

Apolipoproteins do not play a dominant role on any pattern recorded in this work. Their total value is always below 10% of the entire adsorbed proteins. This finding differs significantly from the kinetics results obtained from solid lipid nanoparticles (SLNs), where apolipoproteins played the prominent role on all patterns (Göppert and Müller, 2005). Moreover, it is in agreement with a previous study on iron oxide nanoparticles, where only minor amounts of ApoA-I and ApoA-II have been spotted on the particle surface (Thode et al., 1997). Notable is a certain amount of apoE, as it has shown the ability to deliver drugs across the blood brain barrier (BBB) earlier (Kreuter et al., 2002). Thus, a possible, novel and non-invasive location of USPIO nanoparticles for MRI in the brain might be possible. Certainly, further studies have to prove the principle of this new targeting potential.

Even less is the amount of detected albumin (alike the Vroman kinetics, Section 3.1). This result is not entirely new for iron oxide particles, as Thode et al. (1997) reported similar results for their magnetite samples. The low albumin adsorption is another indicator that the particles will be rapidly removed from the bloodstream, since albumin is known as a protein with dysopsonic behavior (Ogawara et al., 2004).

In summary, a relative stable protein adsorption on superparamagnetic iron oxide nanoparticles over time periods ranging from 0.5 min to 4 h, proved by 2-D PAGE patterns, has been observed. There is little evidence for protein displacement on the surface of the citrate/TREG stabilized iron oxide nanoparticles and therefore, it is easier to predict their in vivo organ distribution.

4. Conclusions

The plasma protein adsorption kinetics on superparamagnetic iron oxide (USPIO) particles was analyzed by two-dimensional polyacrylamide gel electrophoresis (2-D PAGE) in combination with particle incubation in diluted plasma. The results reveal there is no typical Vroman effect on the iron oxide nanoparticles under study. No displacement of previously adsorbed proteins by proteins possessing a higher affinity to the particle surface can be determined. Compared to other nanoparticulate drug delivery systems, similar results have been reported singularly for o/w nanoemulsions, whereas the existence of a Vroman effect has been observed on the surface of polymeric model particles and solid lipid nanoparticles (SLNs). However, there are differences in the protein adsorption patterns received from iron oxide particles compared to o/w nanoemulsions. Immunoglobulins are the dominant protein group during all stages of plasma protein adsorption onto USPIO particles. In addition, an increasing amount of fibrinogen with prolonged incubation times has been observed. Both species belong to the group of opsonic blood proteins, facilitating the macrophages to detect the administered nanoparticles. From this a rapid clearance from the bloodstream and an accumulation mainly in the liver are predicted. Low amounts of adsorbed dysopsonic proteins, such as apolipoproteins and albumin, do support this prediction. Over a certain period of time, minutes to hours, more important for the in vivo behavior of intravenously injected particles, the protein adsorption patterns were qualitatively similar to each other. Furthermore, the relative amount of major proteins, such as apolipoproteins, fibrinogen, and albumin kept constant over time. Singularly, the amount of adsorbed immunoglobulins increased with prolonged incubation times. The knowledge of the protein adsorption patterns and kinetics on USPIO nanoparticles surfaces might be an important step on the way to tailor-made targeted iron oxide nanoparticles. Thus, when processes of protein adsorption and the corresponding body distribution are known, one can design iron oxide nanoparticles with optimized physicochemical surface properties, which are expected to automatically adsorb the proteins required for localization in a certain tissue, i.e. these iron oxide nanoparticles are "self-targeted" to the desired site of action.

Acknowledgements

This work was supported by the German Research Foundation "Deutsche Forschungsgemeinschaft" (DFG), Bonn, Germany (MU708/11-5 and SPP 1313, Cluster NanoSelect (RU420/9-2) and by the priority program of Freie Universität Berlin "Nanoscale Functional Materials".

References

Bio-Rad Silver Staining. Bio-Rad Laboratories. <http://www.bio-rad.com/webroot/web/pdf/lsr/literature/Bulletin_9057.pdf> (accessed 16.11.11), LIT34 Rev B.

Blunk, T., 1994. PhD Thesis – Plasmaproteinadsorption auf kolloidalen Arzneistoffträgern. Christian-Albrechts-Universität, Kiel, Germany.

Blunk, T., Hochstrasser, D.F., Sanchez, J.C., Müller, B.W., Müller, R.H., 1993. Colloidal carriers for intravenous drug targeting: plasma protein adsorption patterns on surface-modified latex particles evaluated by two-dimensional polyacrylamide gel electrophoresis. Electrophoresis 14, 1382–1387.

Blunk, T., Lück, M., Calvor, A., Hochstrasser, D.F., Sanchez, J.-C., Müller, B.W., Müller, R.H., 1996. Kinetics of plasma protein adsorption on model particles for controlled drug delivery and drug targeting. Eur. J. Pharm. Biopharm. 42, 262–268.

Brash, J.L., Ten Hove, P., 1993. Protein adsorption studies on 'standard' polymeric materials. J. Biomater. Sci. Polym. Ed. 4, 591–599.

Cai, W., Wan, J., 2007. Facile synthesis of superparamagnetic magnetite nanoparticles in liquid polyols. J. Colloid Interface Sci. 305, 366–370.

Camner, P., Lundborg, M., Lastbom, L., Gerde, P., Gross, N., Jarstrand, C., 2002. Experimental and calculated parameters on particle phagocytosis by alveolar macrophages. J. Appl. Physiol. 92, 2608–2616.

Capriotti, A.L., Caracciolo, G., Cavaliere, C., Crescenzi, C., Pozzi, D., Lagana, A., 2011. Shotgun proteomic analytical approach for studying proteins adsorbed onto liposome surface. Anal. Bioanal. Chem. 401, 1195–1202.

Cook, B.C., Retzinger, G.S., 1992. Elution of fibrinogen and other plasma proteins from unmodified and from lecithin-coated polystyrene divinylbenzene beads. J. Colloid Interface Sci. 153, 1–12.

Ferrucci, J.T., 1990. Liver tumor imaging: current concepts. AJR Am. J. Roentgenol. 155, 473–484.

Fukuda, Y., Ando, K., Ishikura, R., Kotoura, N., Tsuda, N., Kato, N., Yoshiya, S., Nakao, N., 2006. Superparamagnetic iron oxide (SPIO) MRI contrast agent for bone marrow imaging: differentiating bone metastasis and osteomyelitis. Magn. Reson. Med. Sci. 5, 191–196.

Gasteiger, E., Gattiker, A., Hoogland, C., Ivanyi, I., Appel, R.D., Bairoch, A., 2003. ExPASy: The proteomics server for in-depth protein knowledge and analysis. Nucleic Acids Res. 31, 3784–3788.

Göppert, T.M., Müller, R.H., 2004. Alternative sample preparation prior to two-dimensional electrophoresis protein analysis on solid lipid nanoparticles. Electrophoresis 25, 134–140.

Göppert, T.M., Müller, R.H., 2005. Adsorption kinetics of plasma proteins on solid lipid nanoparticles for drug targeting. Int. J. Pharm. 302, 172–186.

Gupta, A.K., Curtis, A.S., 2004. Surface modified superparamagnetic nanoparticles for drug delivery: interaction studies with human fibroblasts in culture. J. Mater. Sci. Mater. Med. 15, 493–496.

Gupta, A.K., Wells, S., 2004. Surface-modified superparamagnetic nanoparticles for drug delivery: preparation, characterization, and cytotoxicity studies. IEEE Trans. Nanobiosci. 3, 66–73.

Harnisch, S., Müller, R.H., 1998. Plasma protein adsorption patterns on emulsions for parenteral administration: establishment of a protocol for two-dimensional polyacrylamide electrophoresis. Electrophoresis 19, 349–354.

Harnisch, S., Müller, R.H., 2000. Adsorption kinetics of plasma proteins on oil-in-water emulsions for parenteral nutrition. Eur. J. Pharm. Biopharm. 49, 41–46.
Hochstrasser, D.F., Funk, M., Appel, R.D., Pun, T., James, R.W., Hochstrasser, A.C., Scherrer, J.R., Pellegrini, C., Müller, A.F., 1990. From biopsy to automatic diagnosis. Schweiz. Med. Wochenschr. 120, 1862–1866.
Huang, J., Yue, Y., Zheng, C., 1999. Vroman effect of plasma protein adsorption to biomaterials surfaces. Sheng Wu Yi Xue Gong Cheng Xue Za Zhi 16, 371–376.
Ihlenfeld, J.V., Cooper, S.L., 1979. Transient in vivo protein adsorption onto polymeric biomaterials. J. Biomed. Mater. Res. 13, 577–591.
Jorgensen, L., Wood, G.K., Rosenkrands, I., Petersen, C., Christensen, D., 2009. Protein adsorption and displacement at lipid layers determined by total internal reflection fluorescence (TIRF). J. Liposome Res. 19, 99–104.
Kang, S.C., Jo, Y.J., Bak, J.P., Kim, K.C., Kim, Y.S., 2007. Evaluation for protein binding affinity of maghemite and magnetite nanoparticles. J. Nanosci. Nanotechnol. 7, 3706–3708.
Klose, J., Kobalz, U., 1995. Two-dimensional electrophoresis of proteins: an updated protocol and implications for a functional analysis of the genome. Electrophoresis 16, 1034–1059.
Kreuter, J., Shamenkov, D., Petrov, V., Ramge, P., Cychutek, K., Koch-Brandt, C., Alyautdin, R., 2002. Apolipoprotein-mediated transport of nanoparticle-bound drugs across the blood-brain barrier. J. Drug Target. 10, 317–325.
Leroux, J.C., Gravel, P., Balant, L., Volet, B., Anner, B.M., Allemann, E., Doelker, E., Gurny, R., 1994. Internalization of poly(D,L-lactic acid) nanoparticles by isolated human leukocytes and analysis of plasma proteins adsorbed onto the particles. J. Biomed. Mater. Res. 28, 471–481.
Lind, K., Kresse, M., Debus, N.P., Müller, R.H., 2002. A novel formulation for superparamagnetic iron oxide (SPIO) particles enhancing MR lymphography: comparison of physicochemical properties and the in vivo behaviour. J. Drug Target. 10, 221–230.
Lind, K., Kresse, M., Müller, R.H., 2001. Comparison of protein adsorption patterns onto differently charged hydrophilic superparamagnetic iron oxide particles obtained in vitro and ex vivo. Electrophoresis 22, 3514–3521.
Magin, R.L., Bacic, G., Niesman, M.R., Alameda Jr., J.C., Wright, S.M., Swartz, H.M., 1991. Dextran magnetite as a liver contrast agent. Magn. Reson. Med. 20, 1–16.
Merril, C.R., Goldman, D., Sedman, S.A., Ebert, M.H., 1981. Ultrasensitive stain for proteins in polyacrylamide gels shows regional variation in cerebrospinal fluid proteins. Science 211, 1437–1438.
Mientus, W., Knippel, E., 1995. Theoretical modelling of plasma protein adsorption/desorption processes onto solid surfaces. J. Biomater. Sci. Polym. Ed. 7, 401–414.
Moghimi, S.M., Muir, I.S., Illum, L., Davis, S.S., Kolb-Bachofen, V., 1993. Coating particles with a block co-polymer (poloxamine-908) suppresses opsonization but permits the activity of dysopsonins in the serum. Biochim. Biophys. Acta 1179, 157–165.
Müller, R.H., Heinemann, S., 1989. Surface modelling of microparticles as parenteral systems with high tissue affinity. In: Gurny, R., Junginger, H.E. (Eds.), Bioadhesion – Possibilities and Future Trends. Wissenschaftliche Verlagsgesellschaft, Stuttgart, pp. 202–214.
Müller, R.H., Lück, M., Harnisch, S., Thode, K., 1997. Intravenously injected particles; surface properties and interaction with blood proteins – the key determining the organ distribution. In: Schütt, W., Teller, J., Häfeli, U., Zborowski, M. (Eds.), Scientific and Clinical Applications of Magnetic Carriers. Plenum Press, New York, pp. 135–148.
Nagayama, S., Ogawara, K., Fukuoka, Y., Higaki, K., Kimura, T., 2007. Time-dependent changes in opsonin amount associated on nanoparticles alter their hepatic uptake characteristics. Int. J. Pharm. 342, 215–221.
Ogawara, K., Furumoto, K., Nagayama, S., Minato, K., Higaki, K., Kai, T., Kimura, T., 2004. Pre-coating with serum albumin reduces receptor-mediated hepatic disposition of polystyrene nanosphere: implications for rational design of nanoparticles. J. Control. Release 100, 451–455.
Osaka, T., Nakanishi, T., Shanmugam, S., Takahama, S., Zhang, H., 2009. Effect of surface charge of magnetite nanoparticles on their internalization into breast cancer and umbilical vein endothelial cells. Colloids Surf. B Biointerfaces 71, 325–330.
Peng, X.H., Qian, X., Mao, H., Wang, A.Y., Chen, Z.G., Nie, S., Shin, D.M., 2008. Targeted magnetic iron oxide nanoparticles for tumor imaging and therapy. Int. J. Nanomed. 3, 311–321.
Pouliquen, D., Perdrisot, R., Ermias, A., Akoka, S., Jallet, P., Le Jeune, J.J., 1989. Superparamagnetic iron oxide nanoparticles as a liver MRI contrast agent: contribution of microencapsulation to improved biodistribution. Magn. Reson. Imaging 7, 619–627.
Saini, S., Edelman, R.R., Sharma, P., Li, W., Mayo-Smith, W., Slater, G.J., Eisenberg, P.J., Hahn, P.F., 1995. Blood-pool MR contrast material for detection and characterization of focal hepatic lesions: initial clinical experience with ultrasmall superparamagnetic iron oxide (AMI-227). AJR Am. J. Roentgenol. 164, 1147–1152.
Saini, S., Stark, D.D., Hahn, P.F., Wittenberg, J., Brady, T.J., Ferrucci Jr., J.T., 1987. Ferrite particles: a superparamagnetic MR contrast agent for the reticuloendothelial system. Radiology 162, 211–216.
Servoli, E., Maniglio, D., Aguilar, M.R., Motta, A., San Roman, J., Belfiore, L.A., Migliaresi, C., 2008. Quantitative analysis of protein adsorption via atomic force microscopy and surface plasmon resonance. Macromol. Biosci. 8, 1126–1134.
Shen, J.W., Wu, T., Wang, Q., Pan, H.H., 2008. Molecular simulation of protein adsorption and desorption on hydroxyapatite surfaces. Biomaterials 29, 513–532.
Silver, J.H., Lin, H.B., Cooper, S.L., 1993. Effect of protein adsorption on the blood-contacting response of sulphonated polyurethanes. Biomaterials 14, 834–844.
Thode, K., 1996. PhD Thesis – specific contrast agents for magnetic resonance tomography: physico-chemical characterisation and studies on plasma protein adsorption. Freie Universität, Berlin, Germany.
Thode, K., Lück, M., Semmler, W., Müller, R.H., Kresse, M., 1997. Determination of plasma protein adsorption on magnetic iron oxides: sample preparation. Pharm. Res. 14, 905–910.
Tissot, J.D., Schneider, P., James, R.W., Daigneault, R., Hochstrasser, D.F., 1991. High-resolution two-dimensional protein electrophoresis of pathological plasma/serum. Appl. Theor. Electrophor. 2, 7–12.
Vroman, L., 1962. Effect of absorbed proteins on the wettability of hydrophilic and hydrophobic solids. Nature 196, 476–477.
Vroman, L., 1988. The life of an artificial device in contact with blood: initial events and their effect on its final state. Bull. N. Y. Acad. Med. 64, 352–357.
Vroman, L., Adams, A.L., 1986. Adsorption of proteins out of plasma and solutions in narrow spaces. J. Colloid Interface Sci. 111, 391–402.
Vroman, L., Adams, A.L., Fischer, G.C., Munoz, P.C., 1980. Interaction of high molecular weight kininogen, factor XII, and fibrinogen in plasma at interfaces. Blood 55, 156–159.
Weissleder, R., Saini, S., Stark, D.D., Wittenberg, J., Ferrucci, J.T., 1988. Dual-contrast MR imaging of liver cancer in rats. AJR Am. J. Roentgenol. 150, 561–566.
Yang, X., Hong, H., Grailer, J.J., Rowland, I.J., Javadi, A., Hurley, S.A., Xiao, Y., Yang, Y., Zhang, Y., Nickles, R.J., Cai, W., Steeber, D.A., Gong, S., 2011. cRGD-functionalized, DOX-conjugated, and Cu-labeled superparamagnetic iron oxide nanoparticles for targeted anticancer drug delivery and PET/MR imaging. Biomaterials 32, 4151–4160.